Chapter 1

Introduction

1.1 Overview of Vacuum Microelectronics

1.1.1 History of vacuum microelectronics

Nowadays, there has been a growing interest in vacuum microelectronics. Some of the reasons for the increasing interest have to do with the superior theoretical electrical characteristics of the vacuum microelectronic devices over semiconductor devices. Scattering mechanisms, such as electron-phonon scattering and lattice scattering etc., occurred during electron transportation in semiconductor devices no longer exist in vacuum microelectronic devices because of the electrons solely travel in a vacuum environment, which plays a role as an active vacuum channel. Thus, the transit time of the vacuum microelectronic devices will be less than that of semiconductor devices. In addition, since electron field emission mechanism has been applied on vacuum devices to extract electrons from the surface of metal, it is possible for vacuum devices to have a current density greater than that of Bipolar Transistors

(BJTs). Moreover, electrons traveling in the active vacuum channel result in greatly reduced (nearly eliminated) temperature sensitivity problem which usually comes along with semiconductor devices. In order to accomplish better understanding of the advantages of vacuum microelectronic devices, a brief history of the theory of electron field emission and vacuum microelectronic devices is very helpful.

Vacuum tubes have been gradually replaced by solid state electronic devices since solid state transistors in the late 1940s for the tiny volume, low cost, better reliability, and more power efficiency of solid state devices were invented. For the past decades, great improvements on semiconductor manufacturing technology gave a new life to vacuum electronics for the professional micro fabrication process to fabricate tiny vacuum devices, which is now called vacuum microelectronics. “Vacuum state” devices have a great deal of superior advantages as compared with solid-state devices, including fast carrier drift velocity, radiation hardness, and temperature insensitivity. For example, the saturation drift velocity is limited to less than 3×10^{7} cm/s in all semiconductor due to scattering mechanism whereas the saturation drift velocity in vacuum is limited theoretically to 3×10^{10} cm/s and practically to about $6\text{-}9\times10^{8}$ cm/s [1]. Moreover, temporary or permanent radiation effect is negligible in vacuum devices for no medium is being damaged. Additionally, the effect of temperature on performance is reduced in vacuum devices simply

because no medium is causing the temperature effect in semiconductor, such as increased lattice scattering or bulk carrier generation/recombination. Table 1-1 shows the comparison between vacuum microelectronic and semiconductor devices.

Table 1-1 Comparison between vacuum microelectronics and solid-state electronics.

Items	Solid State Microelectronics	Vacuum Microelectronics
Current Density	**10^4 – 10^5 (A/cm^2)**	**similar**
Turn-on Voltage	**0.1 – 0.7 V**	**5 – 300 V**
Structure	**solid/solid interface**	**solid/vacuum interface**
Electron Transport	**in solid**	**in vacuum**
Electron Velocity	**3×10^7 (cm/sec)**	**3×10^{10} (cm/sec)**
Flicker Noise	**due to interface**	**due to emission**
Thermal & Short Noise	**comparable**	**comparable**
Electron Energy	**< 0.3 eV**	**a few to 1000 eV**
Cut-off Frequency	**< 20 GHz (Si) & 100 GHz (GaAs)**	**< 100 – 1000 GHz**
Power	**small – medium**	**medium – large**
Radiation Hardness	**poor**	**excellent**
Temperature Effect	**-30 – 50 °C**	**< 500 °C**
Fabrication & Materials	**well established (Si) & fairly well (GaAs)**	**not well established**

Recent developments in vacuum microelectronics started in 1928, when R. H. Fowler and L. W. Nordheim published the first theory of electron field emission from metals using quantum mechanics [2]. This theory is contrary to thermionic emission, by which metal has to be heated so that some of the electrons in the metal gain enough thermal energy to overcome the metal/vacuum barrier. According to the

Fowler-Nordheim theory, an applied electric field of approximately 10^3 V/μm is needed for electrons to tunnel through the sufficiently narrow barrier [3]. To reach the high field at reasonable applied voltage, producing the field emitters into protruding objects is essential to take advantage of field enhancement. It was not until 1968 when C. A. Spindt came up with a fabrication method to create very small dimension metal cones that vacuum microelectronic triodes became possible [4]. From the late 1960s to the year 1990, Ivor Brodie, Henry F. Gray, and C. A. Spindt made many contributions in this field. Also, most of the research during the past three decades was focused on the devices similar to the Spindt cathode.

In 1991, a group of researchers of the French company LETI CHEN reported a microtip display at the fourth International Vacuum Microelectronics Conference [5]. Their display was the first announcement of a practical vacuum microelectronic device. From then on, lots of researchers all over the world have devoted themselves to this interesting, challenging, and inventive field. Part of the work focused on fabricating very small radius silicon tip by utilizing modern VLSI technology [6-7]. Some of them increased the emission current by coating different metals, such as W, Mo, Ta, Pt etc., even diamond on field emission arrays [8-10]. Different device schemes also have been proposed to enhance the emission current density, stability, and reliability.

1.1.2 Theory Background

Electron field emission is a quantum mechanical tunneling phenomenon of electrons extracted from the conductive solid surface, such as a metal or a semiconductor, where the surface electric field is extremely high. If a sufficient electric field is applied on the emitter surface, electrons will be emitting through the surface potential barrier into vacuum, even under a very low temperature. In contrast, thermionic emission is the hot electron emission under high temperature and low electric field. Fig. 1-1(a) demonstrates the band diagram of a metal-vacuum system.

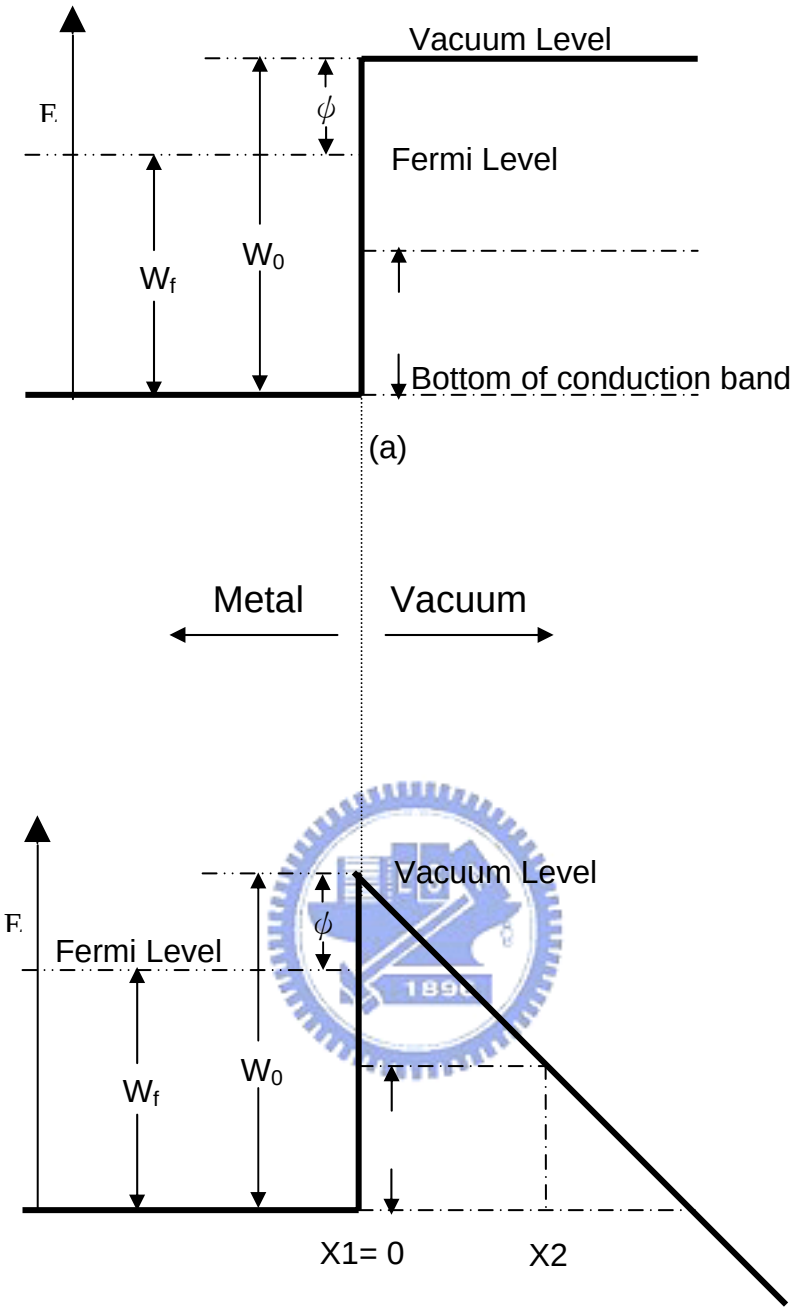

Fig. 1-1 Energy diagrams of vacuum-metal boundary: (a) without external electric field; and (b) with an external electric field.

Here W_0 is the energy difference between an electron at rest outside the metal and an electron at rest inside, whereas W_f is the energy difference between the Fermi level and the bottom of the conduction band. The work function ϕ is defined as $\phi = W_0 - W_f$. If an external bias is applied, vacuum energy level is reduced and the potential barrier at the surface becomes thinner as shown in Fig. 1-1(b). Then, an electron having energy "W" has a finite probability of tunneling through the surface barrier. Fowler and Nordheim derive the famous F-N equation (1.1) as follow [3]:

$$J = \frac{aE^2}{\phi t^2(y)} \exp[-b\phi^{\frac{3}{2}} v(y)/E], \tag{1-1}$$

where J is the current density (A/cm^2). E is the applied electric field (V/cm), ϕ is the work function (in eV), $a = 1.56\times10^{-6}$, $b = -6.831\times10^{-7}$, $y = 3.79x10^{-4}\times10^{-4}E^{1/2}/\phi$, $t^2(y)\sim1.1$ and v(y) can be approximated as [11]

$$v(y) = \cos(0.5\pi y), \tag{1-2}$$

or

$$v(y) = 0.95 - y^2. \tag{1-3}$$

Typically, the field emission current I is measured as a function of the applied voltage V. Substituting relationships of $J = I/\alpha$ and $E = \beta V$ into Eq.(1-1), where α is the emitting area and β is the local field enhancement factor of the emitting surface, the following equation can be obtained

$$I = \frac{A\alpha\beta^2 V^2}{\phi t^2(y)} \exp[-bv(y)\frac{\phi^{\frac{3}{2}}}{\beta V}]. \quad (1\text{-}4)$$

Then taking the log. form of Eq. (1-4) and v(y) ~ 1

$$\log(\frac{I}{V^2}) = \log[1.54\times10^{-6}\frac{\alpha\beta^2}{\phi t^2(y)}] - 2.97\times10^7(\frac{\phi^{3/2}v(y)}{\beta V}), \quad (1\text{-}5)$$

from Eq. (1-5), the slope of a Fowler-Nordheim (F-N) plot is given by

$$S \equiv slope_{FN} = 2.97\times10^7(\frac{\phi^{\frac{3}{2}}}{\beta}), \quad (1\text{-}6)$$

The parameter β can be evaluated from the slope S of the measured F-N plot if the work function ϕ was known

$$\beta = -2.97\times10^7(\frac{\phi^{\frac{3}{2}}}{S}) \quad (\text{cm}^{-1}), \quad (1\text{-}7)$$

The emission area α can be subsequently extracted from a rearrangement of Eq. (1-5)

$$\alpha = (\frac{I}{V^2})\frac{\phi}{1.4\times10^{-6}\beta^2}\exp(\frac{-9.89}{\sqrt{\phi}})\exp(\frac{6.53\times10^7\phi^{\frac{3}{2}}}{\beta V}) \quad (\text{cm}^2). \quad (1\text{-}8)$$

For example, the electric field at the surface of a spherical emitter of radius r concentric with a spherical anode (or gate) of radius r+d can be represented analytically by

$$E = \frac{V}{r}(\frac{r+d}{d}), \quad (1\text{-}9)$$

Though a realistic electric field in the emitter tip is more complicated than above equation, we can multiply Eq.(1-9) by a geometric factor $\beta`$ to approximate the real condition.

$$E_{tip} \equiv \text{function of (r,d)} = \beta` \frac{V}{r}(\frac{r+d}{d}), \quad (1\text{-}10)$$

where r is the tip radius of emitter tip, d is the emitter-anode(gate) distance and $\beta`$ is a geometric correction factor [12].

For a very sharp conical tip emitter, where d >> r, E_{tip} approaches to $\beta`(V/r)$. And for r>>d, $E_{tip}$ approaches to $\beta`(V/d)$ which is the solution for a parallel-plate capacitor and for a diode operation in a small anode-to-cathode spacing.

As the gated FEA with very sharp tip radius, Eq. (1-10) can be approximated as:

$$E_{tip} = \beta`(V/r). \quad (1\text{-}11)$$

Combining E = βV and Eq. (1-11), we can obtain the relationship:

$$E_{tip} = \beta V = \beta`(V/r), \text{ and } \beta` = \beta r. \quad (1\text{-}12)$$

The tip radius r is usually in the range from a few nm to 50 nm, corresponding to the parameter $\beta`$ ranging from 10^{-1} to 10^{-2}.

Besides, transconductance g_m of a field emission device is defined as the change in anode current due to the change in gate voltage [1].

$$g_m = \frac{\partial I_C}{\partial V_g}|_{Vc}, \qquad (1\text{-}13)$$

Transconductance of a FED is a figure of merit that gives as an indication of the amount of current charge that can be accomplished by a given change in grid voltage. The transconductance can be increased by using multiple tips or by decreasing the gate-to-cathode spacing for a given anode-to-cathode spacing.

According to the equations above mentioned (especially Eq.1-5), the following approaches may therefore be taken to reduce the operating voltage of the field emission devices:

1) Find techniques to reproducibly sharpen the tips to the atomic level (increase β).

2) Lower the work function of the tip (ϕ).

3) Narrow the cone angle (increase β).

4) Reduce the gate-opening diameter (increase β).

1.2 Applications of Vacuum Microelectronic Devices

Because of the superior properties of vacuum microelectronic devices, potential

applications include high brightness flat-panel display [13-17], high efficiency microwave amplifier and generator [18-20], ultra-fast computer, intense electron/ion sources [21-22], scanning electron microscopy, electron beam lithography, micro-sensor [23-24], temperature insensitive electronics, and radiation hardness analog and digital circuits.

1.2.1 Vacuum Microelectronic Devices for Electronic Circuits

Either vacuum or solid-state devices can generate power at frequencies in the GHz range. Solid-state devices, such as impact avalanche transit time (IMPATT) diodes, Si bipolar transistors, and GaAs FETs [25], are typically used in the lower power (up to 10 W) and frequency (up to 10 GHz) range. Vacuum devices still remain the only technology available for high power and high frequency applications. These devices include traditional multi-terminal vacuum tubes, like triodes, pentodes, and beam power tubes, and distributed-interaction devices, such as traveling wave tubes (TWTs), klystrons, backward-wave oscillators (BWOs).

The performance of FEAs in conventionally modulated power tubes, like TWT, is determined primarily by their emission current and current density capability. On the other hand, the application of FEAs in the microwave tubes in which modulation of

the beam is accomplished via modulation of the emission current at source, such as capacitance and transconductance. Successful operation of a gated FEA in a 10 GHz TWT amplifier with conventional modulation of electron beam has been demonstrated by NEC Corporation of Japan [26]. The amplifier employed a modified Spindt-type Mo cathode with circular emission area of 840 μm in diameter. The modified cathode structure incorporated a resistive poly-Si layer as a current limiting element. The emission current from the cathode was 58.6 mA. The prototype TWT could operate at 10.5 GHz with the output power of 27.5 W and the gain of 19.5 dB. The bandwidth of the tube was greater than 3 GHz. The prototype was operated for 250 h.

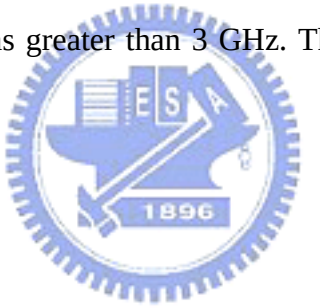

1.2.2 Field Emission Displays

Among wide range applications of the vacuum microelectronics, the first commercial product could be the field emission flat-panel display. The field emission fluorescent display is basically a thin cathode ray tube (CRT), which was first proposed by SRI International and later demonstrated by LETI [5].

Various kinds of flat-panel displays, such as liquid crystal display (LCD), electroluminescent display (EL), vacuum fluorescent display (VFD), plasma display

panel (PDP), and light emitting display (LED), are developed for the better characteristics of small volume, light weight, and low power consumption. LCDs have become the most popular flat panel displays. However, they have some drawbacks, such as poor viewing angle, temperature sensitivity and low brightness. As a result, there are still some opportunities for the solutions from other flat panel displays such as FED.

FED features all the pros of the CRTs in image quality and is flat and small volume. The schematic comparisons are revealed in Fig.1-2. The operation of CRTs involves deflection of the beam in such a way that the electron spot scans the screen line-by-line. In FEDs, multiple electron beams are generated from the field emission cathode and no scanning of beams is required. The cathode is a part of the panel substrate which consists of an X-Y electrically addressable matrix of field emission arrays (FEAs). Each FEA is located at the intersection of a row and a column conductor, with the row conductor serving as the gate electrode and the column conductor as the emitter base. The locations where the rows and columns intersect define a pixel. The pixel area and the number of tips are determined by the desired resolution and luminance of the display. Typically, each pixel contains an FEA of 4-5000 tips. The emission current required for a pixel varies from 0.1 to 10 μA, depending on the factors such as the luminance of the display, phosphor efficiency

and the anode voltage.

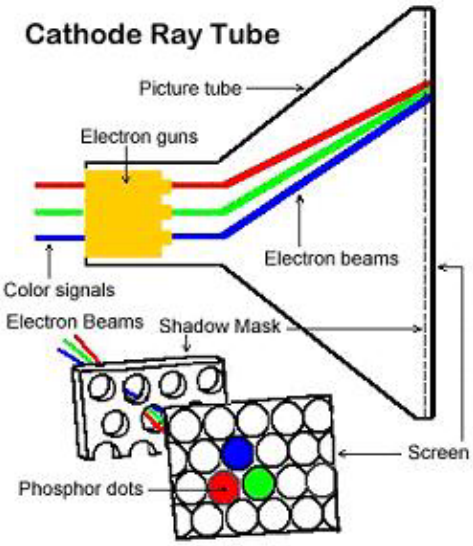

(a)

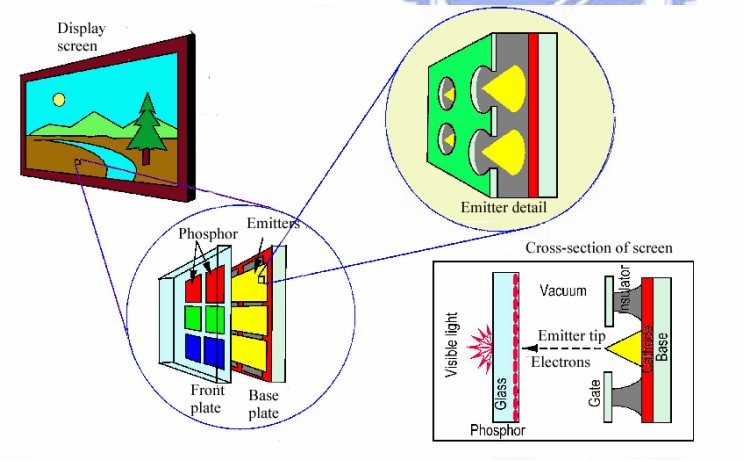

(b)

Fig. 1-2 The schematic diagram of (a) conventional CRT, (b) FED.

Compared to the active matrix LCDs, FEDs generate three times the brightness with wilder viewing angle at the same power level. Full color FEDs have been

developed by various research groups from different aspects such as PixTech, Futaba, Fujitsu, Samsung, are presently engaged in commercially exploiting FED.

1.3 Recent Developments of Field Emission Devices for Field Emission Displays

FED is one of the most promising emissive type flat-panel displays, which can overcome the drawbacks of TFT-LCD. However, some difficult technological subjects should be considered such as microfabrication of cathodes, assembly technology with accuracy of micrometer level, packaging of vacuum panel with thin-glass substrates, vacuum technology to keep stable field emission in small space of flat panels, selection of suitable materials to keep a high vacuum condition in panels and high efficiency phosphor materials. The researching objects of this thesis are to produce novel cathode structure and synthesis of novel emitter materials for FED operations. The experimental background is introduced in the following sections.

1.3.1 Cathode Structures and Materials for Field Emission Displays

A. Spindt-type field emitters

Fig. 1-3 demonstrated the scanning electron microscope (SEM) image of a

spindt type field emission triode [27], which was invented by Spindt of SRI and improved for the electron source of high-speed switching devices or microwave devices [28]. Meyer of LETI presented the capability of using Spindt-type emitters for a display in 1970s [29] and stabilized the field emission from Spindt-type emitters by introducing a resistive layer as the feedback resistance. This proposal triggered the development of field emitters as an electron source of displays by researchers and electronics makers in 1990. The merits of the Spindt type field emitters are summarized as follows: (1) High emission current efficiency, more than 98% anode current to cathode current can be achieved for the symmetric structure of Spindt tip and the gate hole, the lateral electric field to the metal tip can be cancelled out. (2) The fabrication is self-aligned, easy process; uniform field emission arrays can be fabricated easily. Some research groups have successfully fabricated commercial FED products based on Spindt type field emitters such as Futaba, Sony/Candesent, Futaba and Pixtech.[30], and the products above mentioned companies are shown in Fig.1-4.

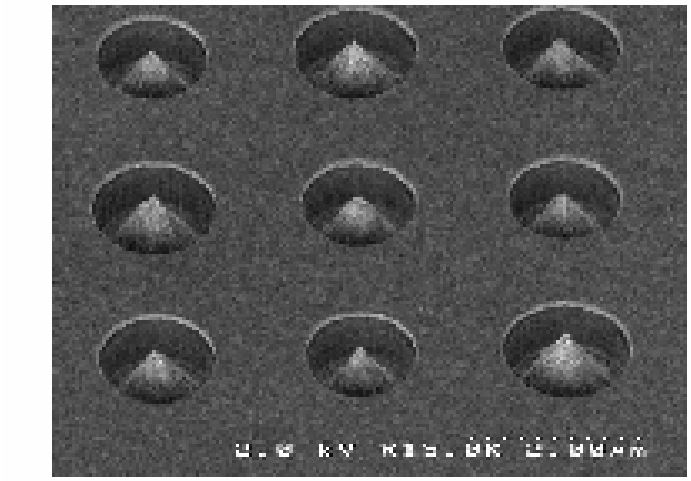

(a)

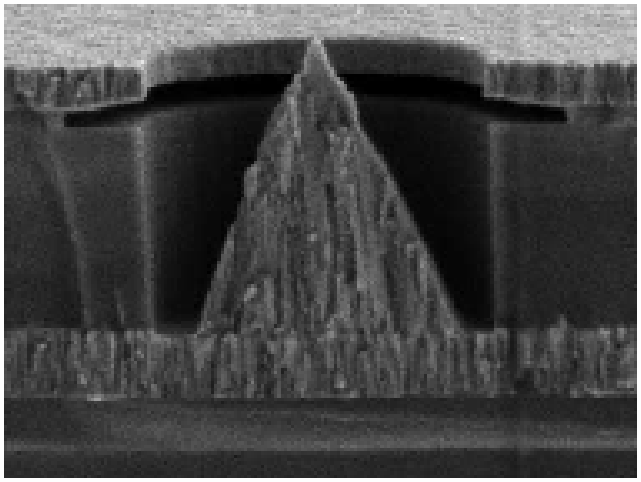

(b)

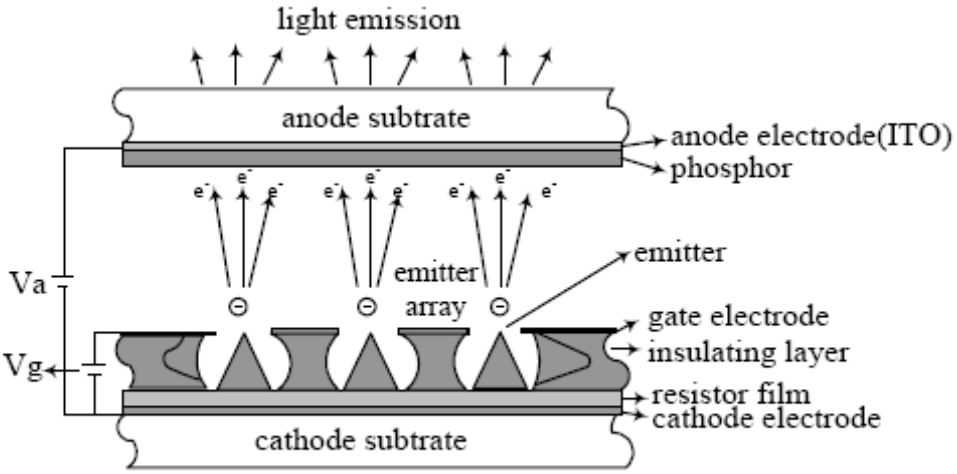

(c)

Fig. 1-3 The SEM micrograph of (a)Spindt type triodes array, (b) Spindt type field

emission triode, and the schematic image of (c) Spindt type triode diagram[27-29]

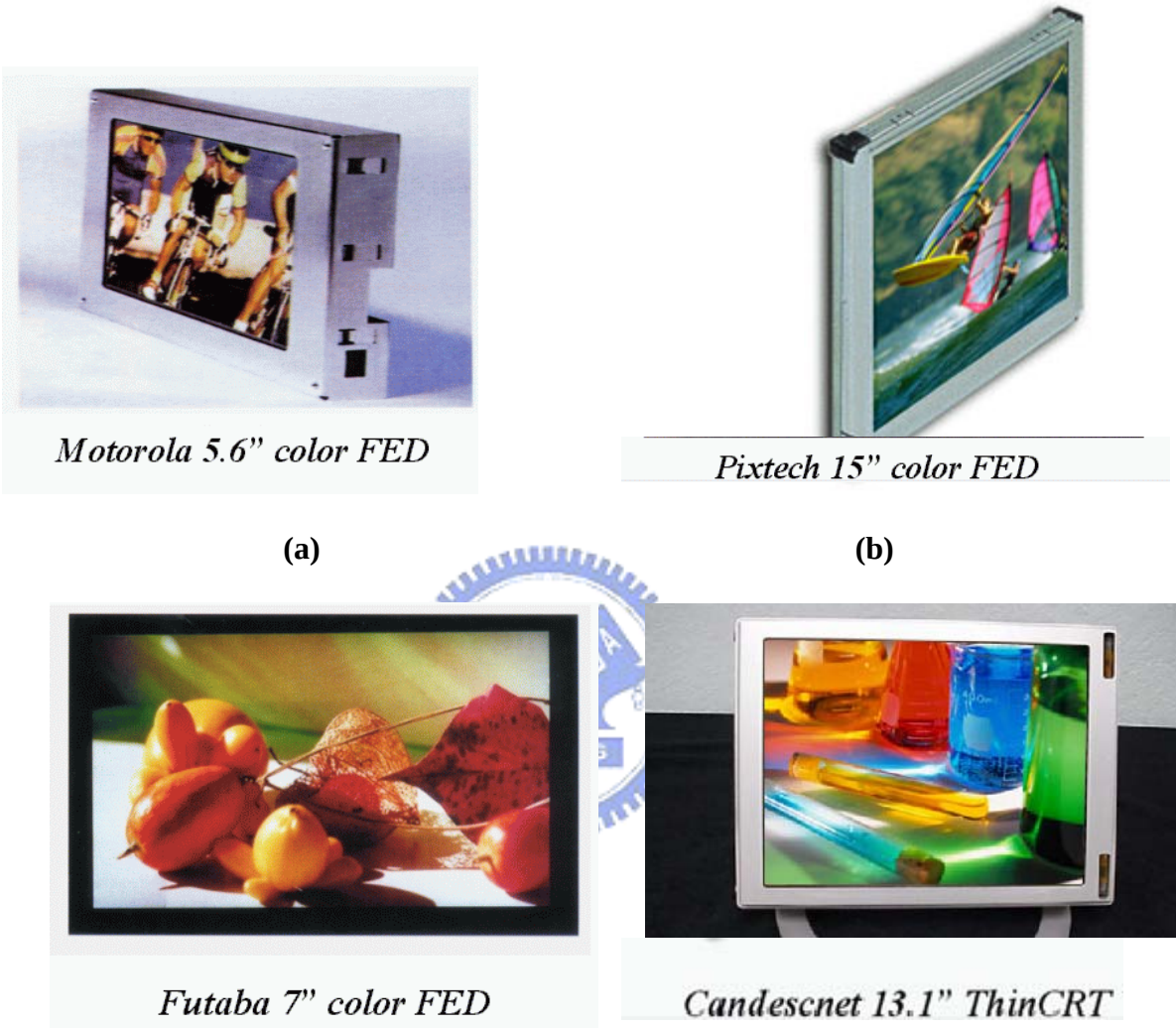

Fig. 1-4 The FED products based on Spindt type field emitters, (a) motorola 5.6" color FED, (b) Pixtech 5.6" color FED,(c) Futaba 7" color FED and (d) Sony/Candescent 13.2" color FED. [30]

However, there are some existing drawbacks of Spindt type field emitters

when fabricating Spindt type FED such as (1) High gate driving voltage required; for a Spindt type field emission triode with 4 μm gate aperture, the driving voltage is typically more than 60 V, which results in the high cost of the driving circuits. To reduce the gate driving voltage, frontier lithography technologies such as E beam lithography must be applied to reduce the gate aperture to the sub-micron level. (2) The emission property degrades for the chemically instable of the metal tips. (3) Huge, expensive high vacuum deposition system required during fabricating large area Spindt type FED.

B. Si tip field emitters

An alternative approach to fabricate tip type field emitters is to fabricate the Si tip field emitters based on the semiconductor fabricating process. Fig. 1-5(a) and (b) depict the SEM micrographs of Si tips array and Si tip field emission triodes array formed by chemical mechanical polishing (CMP) [31] Symmetric device structure and similar advantages with Spindt type field emitters can be obtained. However, high temperature oxidation sharpening process [6] prohibits Si tip from large area fabrication.

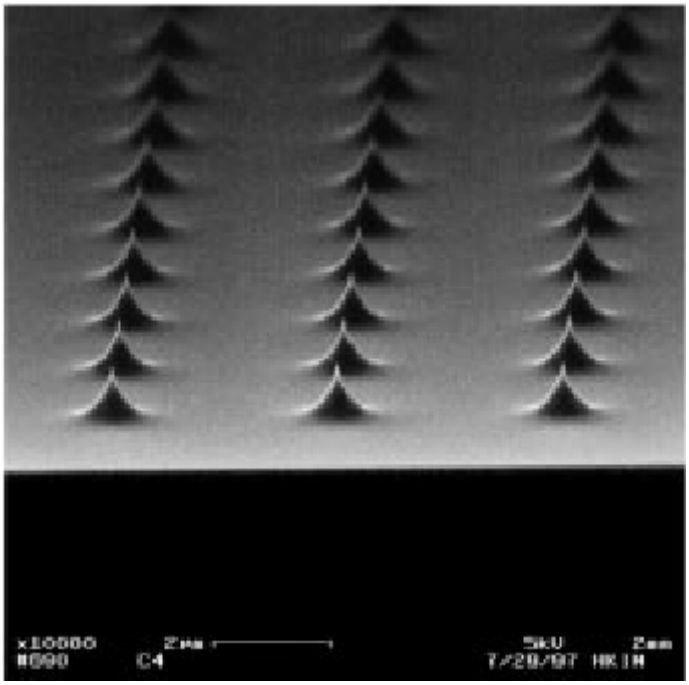

(a)

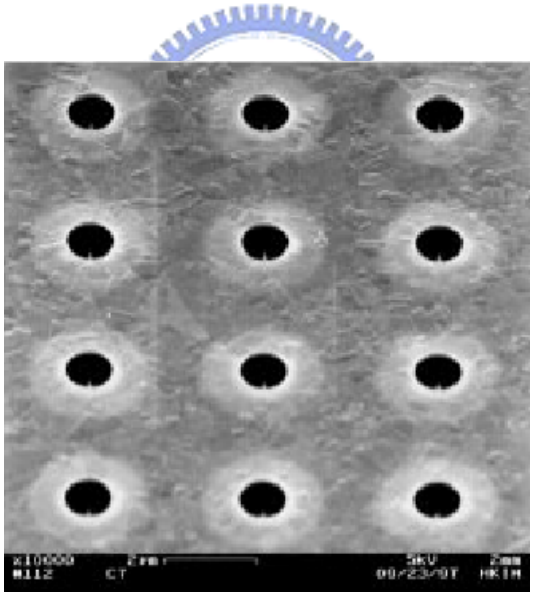

(b)

Fig. 1-5 (a) Si tip formed by isotropic etching and (b) Si tip field emission triodes array formed by CMP. [31]

C. Carbon and Nano-sized Emitters

Carbon nanotubes have attracted a great deal of interests owing to their advantageous properties, such as high aspect ratios, small tip radius of curvature, high Young's modulus, capability for the storage of a large amount of hydrogen, and structural diversities that make it possible for band gap engineering. These useful properties of carbon nanotubes (CNTs) make themselves good candidates for various applications, such as wires for nanosized electronic devices, super strong cables, AFM tips, charge-storage devices in battery, and field emission display.

According to Fowler-Nodheim theory, the electric field at the apex of a needle-shaped tip is enhanced by a factor $\beta = h/r$, where h is the height of the tip and r is the radius of curvature of the tip apex. The carbon nanotube is a stable form of carbon and can be synthesized by several techniques. They are typically made as threads about 10-100 nm in diameter with a high aspect ratio (>1000). These geometric properties, coupled with their high mechanical strength and chemical stability, make carbon nanotubes attractive as electron field emitters. Several research groups have recently reported good electron field emission from nanotubes [32-34].

In 1999, Samsung announced a 4.5-inch carbon nanotube based field emission display. They mixed a conglomeration of single-walled CNTs into a paste with a

nitrocellulose binder and squeezed the concoction through a 20-μm mesh onto a series of metal strips mounted on a glass plate. As emerged from the mesh, the CNTS were forced into a vertical position. The metal strips with the CNTs sticking out of themselves served as the back of the display. The front of the display was a glass plate containing red, green, and blue phosphors and strips of a transparent indium-tin-oxide anode running from side to side. The glass plates were separated by spacers with the thickness of 200 μm. Once assembled, the edges were sealed and air was pumped out of the display.

Samsung's field emission display (Fig. 1-6) could be the precursor of a new generation of more energy efficiency, high performance flat panel displays for portable computers [35]. The CNTs appear to be durable enough to provide the 10000hr lifetime considered a minimum for an electronic product. The panel consumes just half the power of an LCD to generate an equivalent level of screen brightness. They could also be cheaper than LCDs or other types of field emission displays being developed. Until now, at least five major Japanese electronics manufacturers are working on this technology.

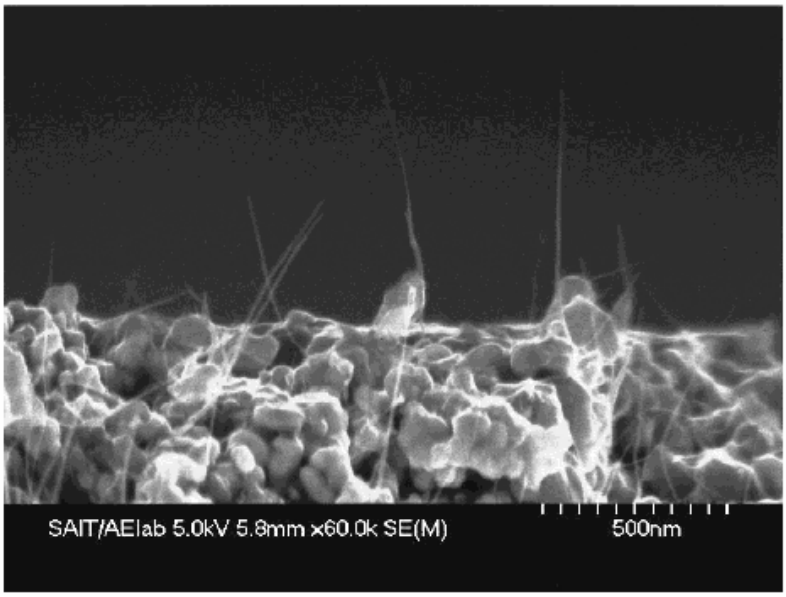

(a)

(b)

Fig. 1-6 (a) SEM image of CNT cathode from Samsung's FED. (b) Demonstration of a 4.5-inch FED from Samsung. The emitting image of fully sealed SWNT-FED at color mode with red, green, and blue phosphor columns. [35]

1.4 Motivation

Due to their interesting field emission properties, carbon nanotubes (CNTs) are currently being actively investigated. While significant progress has been achieved in this field, the experimental theoretical simulation works show that the peculiarities of the emission from CNTs cannot be explained by the corresponding catalytic growth process only .

Various mechanisms have been proposed for the formation of filamentous carbon deposits, whenever for single wall or multiwall nanotubes. Most of the existing models for CVD growth of carbon nanotubes are based on the following model first proposed by Baker: [36] the hydrocarbon molecules decompose at the catalyst surface, and the carbon atoms dissolve into the metal forming a solid solution. When this solution becomes supersaturated, carbon atoms diffusing through the bulk of the particle precipitate at its surface in crystalline graphitic layer. Base and tip growth mechanisms have been proposed, depending on the position of the catalytic particle, which describes how the carbon layers form the tubebody. [37-38] A second group of models focus on the diffusion of carbon at the surface of the metal particle rather than on bulk diffusion.[39]

Despite the large effort to explain CNT growth, the role of the metal catalyst in the formation of the nanoutbes has not been completely clarified. According to Derbyshire et al.,[40] metals from group VI and/or VIII can dissolve a nongraphitic

form of carbon and precipitate carbon as graphite when cooled, or as a consequence of supersaturation. By the words, the catalytic metal acts as a transporting medium.

We investigated the “nano-size” method to accomplish carbon nanotube growth at low temperature because this method has three advantages from paper survey. First, nano-size catalyst particles are more active compared to bulk catalyst metals and exhibit the nano-phenomenon effectively as the Fig.1-7. [41]Second, the melting point decreases as the catalyst particle sizes decrease as the Fig.1-8(a).In particular, K.K.Nanda et al.[42] published the model for the relationship between melting point and particle size. (Co metal for example.)

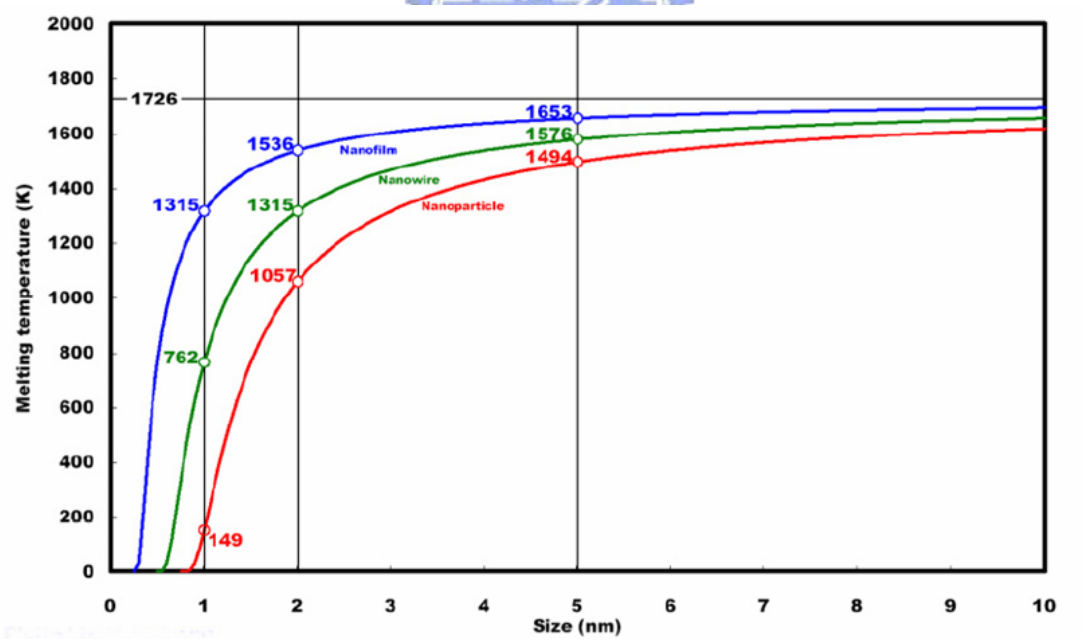

Fig. 1-7 Lindemann criterion [41]

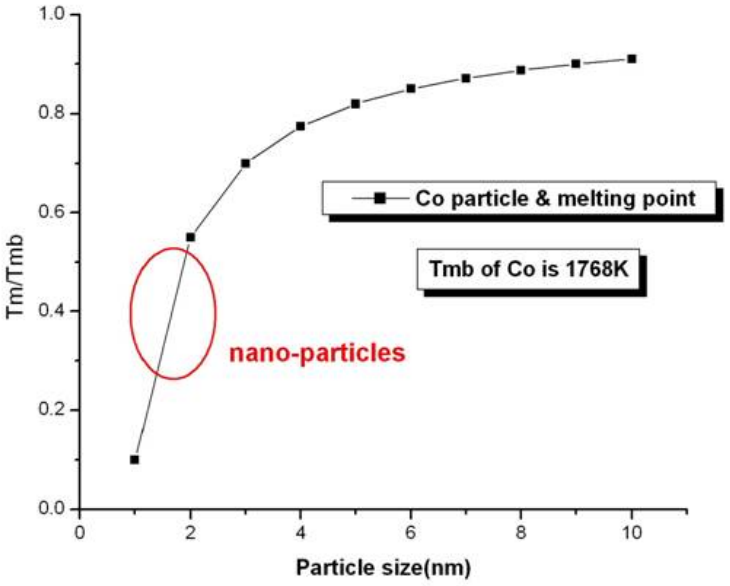

(a)

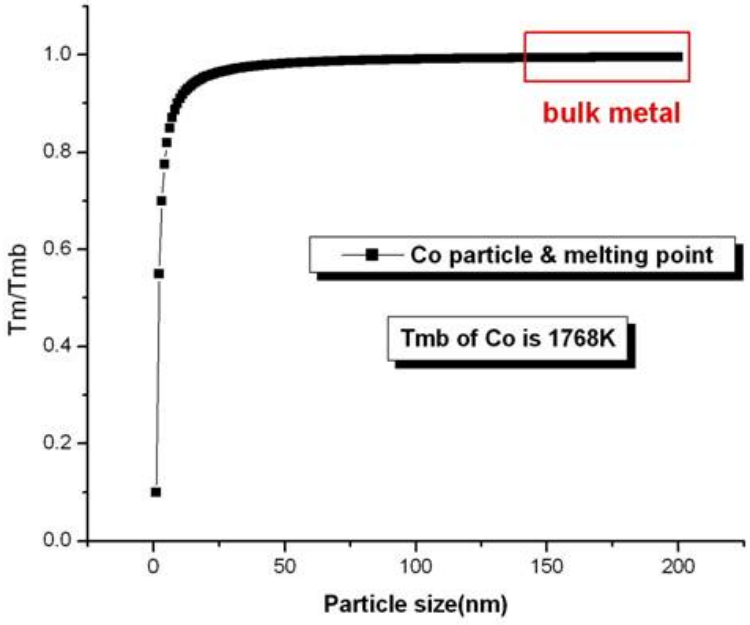

(b)

Fig. 1-8 the relationship between melting point and (a) particle sizes, (b) bulk metal…., Co metal for example [42]

The surface energy was the fundamental electronic properties of a metallic surface, and their determination is of great importance in the understanding of a wide range of surface phenomena. This includes growth rate, the form of crystallites, sintering, catalytic behavior, adsorption, surface segregation, and the formation of grain boundaries. That is, for instance, true for the surface energies derived from the surface tension of liquid metals and listed by de Boer et al [43]. We supposed that the multilayer catalyst films which can form nano-particles have the advantages and synthesized the carbon nanotubes at low temperature via specified interlayer with suitable surface energy.Fig.1-9.

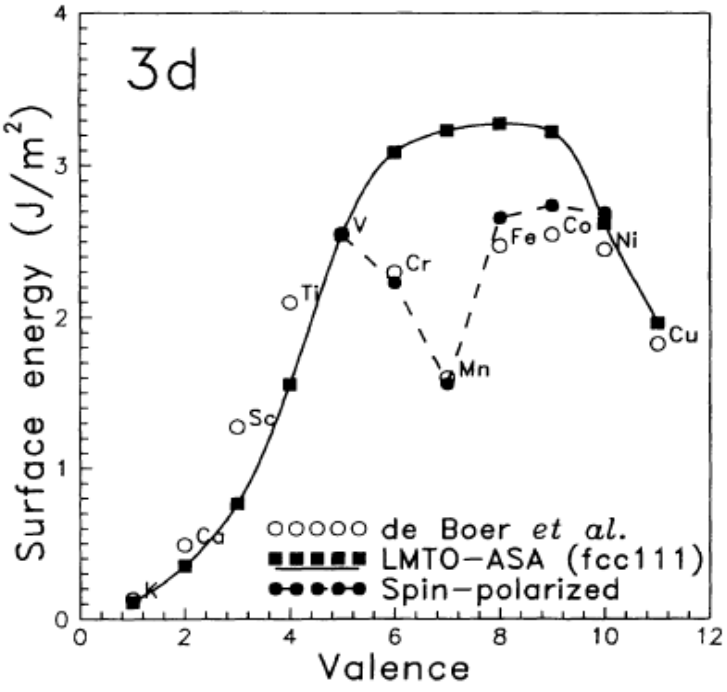

(a)

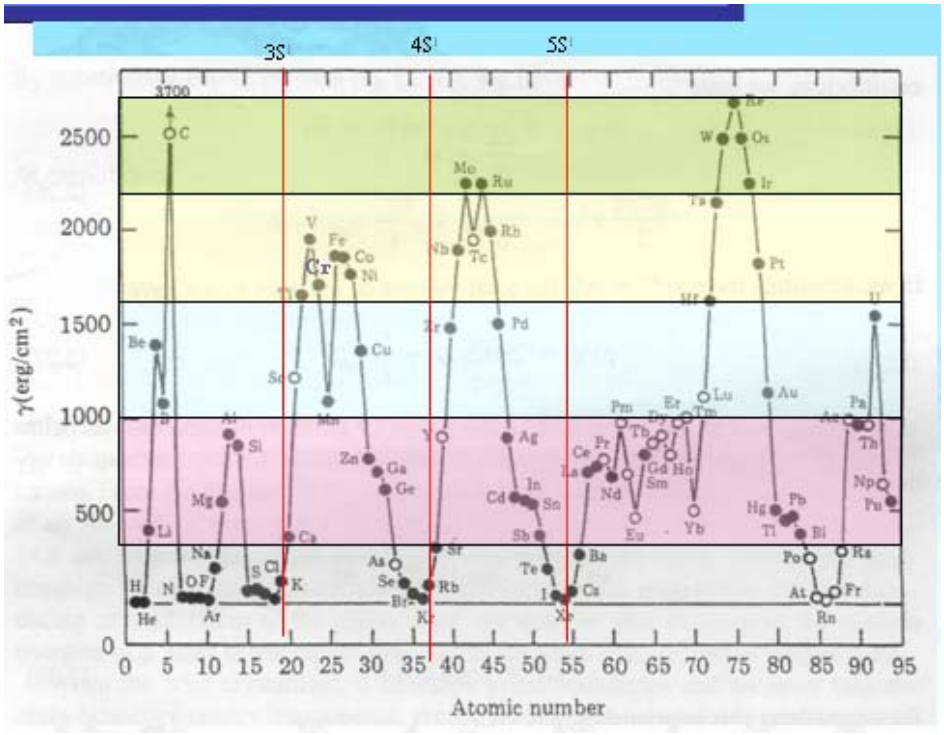

(b)

Fig.1-9 the calculated surface energy for (a) the fcc (111) surfaces of the 3d metals .(b) period tale elements. [43]

In this thesis, different kinds of multilayer catalyst films are synthesized using Thermal chemical vapor deposition (Thermal-CVD) because of its simplicity and low cost unlike other CVD processes and the field emission properties of the CNTs were also investigated. Furthermore, a novel method for improving CNTs growth at low temperature utilized to overcome the Thermal-CVD slowly growth rate, Fig.1-10.[44] was also proposed in this thesis.

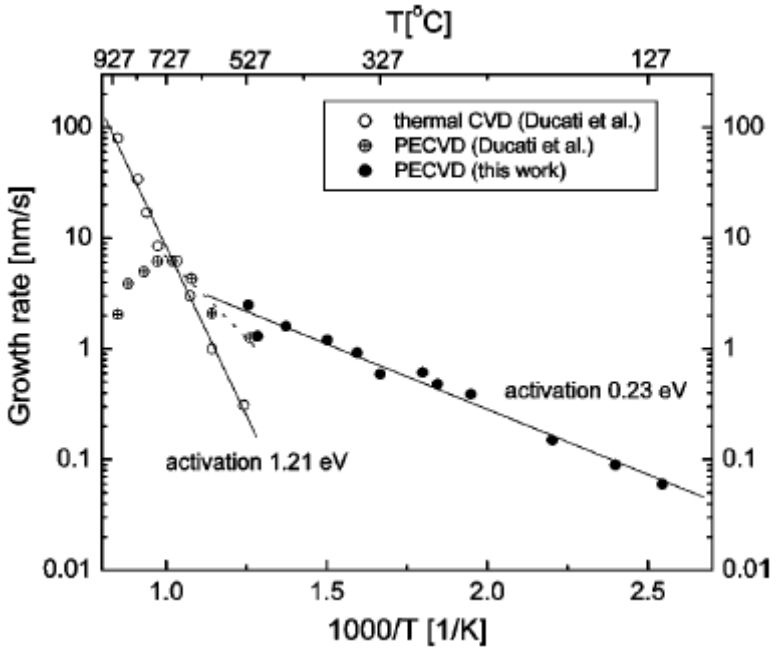

Fig. 1-10 The growth rate variation with temperature for thermal CVD and PECVD. The data points for thermal CVD and high temperature PECVD are from previous data by Ducati *et al.*. The values for the activation energies were calculated from a linear interpolation of the slopes. [44]

Additionally, the improvement of gate controlled anode current CNT-triodes was proposed and characterized. Finally, CNTs were grown on glass substrate for FED application.

1.5 Thesis Organization

The overview of vacuum microelectronics and basic principles of field emission theory was described in chapter 1.

Improvement of the field emission characteristics of carbon nanotubes by

multilayer catalysts on silicon substrate at low temperature and pattern dimension were revealed in chapter 2.

Simple thermal catalytic-CVD method via careful selection of the interlayer is chosen on which the thin catalyst layer is deposited, it was found that the interlayer can tune the shapes and sizes of the catalyst particles, which are controlled by the relative surface energies of the interlayer. Previously, efforts have been made to optimize CNTs growth process by adding a metal multilayer below the catalyst layer, then, the insulated gate structure field emission triodes can avoid the short circuit problem between cathode and gate were also demonstrated. For the filed emission display application, CNTs grown on glass substrate becomes the trend, In order to improve the uniformity of screen printing, there must be an effective process for CNTs grown at low temperature by thermal CVD. CNTs grown on Si and glass substrate show different morphology, so the stability of CNT characteristics, including morphology and field emission properties on glass substrate were presented in chapter 3.

Finally, the conclusions and recommendations for future researches are provided in chapter 4.